Phase formation in Mg-Sn-Zn alloys — thermodynamic calculations vs experimental verification

M. BAMBERGER
Department of Materials Eng., Technion, Haifa, Israel
E-mail: mtrbam@tx.technion.ac.il

Published online: 9 March 2006

Alloy development requires investing huge efforts in the selection of the alloying elements and in the determination of potential compositions and their heat treatments. This effort can be reduced by "intelligent" selection of alloys and processing based on thermodynamic considerations. As an example, we would like to report on the design of heat-treatable Al-free Mg-based alloys, their heat treatment and on the expected precipitation phases during aging following solution treatment as well as exposure to elevated temperatures without precedent heat treatment. The thermodynamically predicted phase formation will be compared with experimental results.

1. Introduction

The worldwide consumption of Mg alloys for the automotive industry has grown very rapidly over the last decade. The main increase is in non heat-treatable High-Pressure-Die-Casting Mg-Al based alloys. Further increase in the consumption of Mg alloys, especially for heavy-duty components, depends on the availability of new Mg-alloys and new processing technologies. Currently, sand casting and gravity die-casting are receiving increased interest, due to the ability to cast and heat-treat heavy-section components which yields improved mechanical properties and structural stability. In this framework, Mg-based alloys with reduced Al contents were investigated [1–5]. When designing the materials and processing, computational thermodynamics offers a powerful tool to reduce the experimental effort and costs involved in the development of new alloys. This approach was used in the investigation of Mg-Al based alloys [6, 7] and their modifications with Ca [8], and Sr [9]. Thermodynamic assessment of the Mg-Mn-Sc [10], Mg-Ce-Al [11], Mg-Ca-Zn [12], Mg-Ca-Si [13], Mg-Al-Ca [14], Mg-Al-Zn [15] and Mg-Al-Ca [16] systems has contributed to better understanding of the physical metallurgy of commercial alloys and to the development of new heat-treatable alloys.

When developing a new Mg alloy, one has to consider the castability of the alloy, in comparison with commercial cast alloys. The die-cast Mg-alloys of the AZ and AM series exhibit a solid-liquid mushy zone (at equilibrium) of 180–200°C [17]. The grain boundary eutectic in AZ91, for example, comprises about 15% of the casting. Therefore, the required characteristics of the investigated heat-treatable Mg-alloy are as follows:

1. Solid-liquid mushy zone (at equilibrium) similar to that of AZ91 to ensure reasonable castability.
2. About 10% of eutectic to reduce the susceptibility to hot-cracking [18].
3. Single phase region of α(hcp)Mg to permit solution treatment at high temperature.
4. Precipitation of intermetallics at elevated temperatures necessary for precipitation hardening.

The application of computational thermodynamics in the design of heat-treatable Mg-alloys, which fulfill the above-mentioned requirements, as well as in the determination of appropriate heat treatment, will be presented below. The expected solid-state reactions and precipitations during aging of solution treated samples, and during the exposure to elevated temperatures of specimens in the as-cast state without prior solution treatment will be discussed and compared with experimental results.

2. Thermodynamic background

The major alloying elements in commercial Mg alloys are Al, and Zn. Recently significant amounts of Sn have been added in newly developed Mg-alloys [19]. Other minor elements, such as Ca, Ce, Nd, Si, Sr, Y and Zr, are commonly used in various Mg alloys. The following

0022-2461
DOI: 10.1007/s10853-006-6294-4

will focus on the ternary system Mg-Zn- Sn with small addition of Ca.

The basis for the calculation of the ternary system Mg-Zn-Sn is the thermodynamic description of the three edge binary-diagrams shown in Fig. 1 and Table I. Published thermochemical and equilibrium data for the edge binary-diagrams were adapted to compile the thermodynamic description of the compounds presented in the edge binary systems listed in Table I [20–24]. The values listed in Table I were adjusted to accommodate recent experimental results.The calculations were performed using ThermoCalc software and a Mg database, Mg 17r15.TDB, including 16 additional elements that has been developed over the past eight years by iteration of computation and experimental studies of multicomponent alloys.The Mg-Sn-Zn description shows the binary Redlich-Kister coefficients for the liquid,hcp and bct solution phases as well as the relevant binary compounds. The reference state for each of the pure elements are defined in terms of the GHSER functions for the pure elements [20], This function is defined as the difference in gibbs energy at one atmosphere for that element in the stable structure and 298.15 K and any temperature above that temperature. In Table I GHSERMG, GHSERZN and GHSERSN refer to the above mentioned functions for hcp Mg and Zn and for bct Sn [20].Thus the compound parameters displayed in Table I are used to approximate the gibbs energies of formation of the various compounds listed from the forms of the stable forms that are stable at 298.15 K. Similarly the Redlich-Kister coefficients listed in Table I for the liquid,hcp and bct phases of the subject edge binaries can be used to define the excess gibbs energies of the substitutional liquid,hcp and bct phases in the Mg-Sn-Zn system as explicit functions of temperature and composition.The latter facility permits calculation of binary,ternary and multicomponent phase diagrams containing these elements using the ThermoCalc software.

The gibbs energy of CaMgSn was not found in the literature and hence it must be estimated based on the following descriptions of the gibbs energy of the following binary compounds:

$$Mg_{0.667}Ca_{0.333} = -9900 + 0.667 * GHSERMG + 0.333 * GHSERCA \text{ J/g at} \quad (1)$$

$$Mg_{0.667}Sn_{0.333} = -26900 + 4.9\,T + 0.667 * GHSERMG + 0.333 * GHSERSN \text{ J/g at} \quad (2)$$

$$Ca_{0.5}Sn_{0.5} = -79500 + 27.5\,T + 0.5 * GHSERCA + 0.5 * GHSERSN \text{ J/g at} \quad (3)$$

$$Ca_{0.667}Sn_{0.333} = -59300 + 14\,T + 0.667 * GHSERCA + 0.333 * GHSERSN \text{ J/g at} \quad (4)$$

TABLE I List of thermodynamic parameters used to calculate the edge binary systems for the Mg-Sn-Zn ternary system (Gibbs Energy in J/gat = J/Mol of atoms,*T* degrees K)

Redlich-Kister Parameters for the Mg-Sn Binary System
L(Liquid,Mg,Sn;0) = −50000−7.5∗T
L(Liquid,Mg,Sn;1) = −21000+10∗T
L(Liquid,Mg,Sn;2) = 20∗T
L(Liquid,Mg,Sn;1) = −63∗T
Redlich-Kister Parameters for the Mg-Zn Binary System
L(Liquid,Mg,Zn;0) = −25400+11.5∗T
L(hcp,Mg,Zn;0) = 3000
Redlich-Kister Parameters for the Sn-Zn Binary System
L(Liquid,Sn,Zn;0) = 13400-8.91∗T
L(Liquid,Sn,Zn;1) = −4400+2.8∗T
L(hcp,Sn,Zn;0) = 20000
L(bct,Sn,Zn;0) = 17000
Compound Phase Parameters for the Mg-Zn System
$G(Mg_{0.7}Zn_{0.3})$= −1092-6∗T+0.7∗GHSERMG +0.3∗GHSERZN
$G(Mg_{0.5}Zn_{0.5})$= −10500+5∗T+0.5∗GHSERMG +0.5∗GHSERZN
$G(Mg_{0.4}Zn_{0.6})$= −10500+2.62∗T+0.4∗GHSERMG +0.6∗GHSERZN
$G(Mg_{0.333}Zn_{0.667})$= −10500+1.7∗T+0.333∗GHSERMG +0.667∗GHSERZN
Compound Phase Parameters for the Mg-Sn System
$G(Mg_{0.667}Sn_{0.333})$= −26900+4.9∗T+0.667∗GHSERMG +0.333∗GHSERSN
GHSER is the gibbs energy difference between 298.15K and a higher temperature T (at a pressure of one atmosphere) for the pure element [20] in the structure stable at 298.15 K
In a recent publication [25] −4.746 ± 0.334 J/gat K is given as the Gibbs free energy of $Mg_{0.667}Sn_{0.333}$ at 298 K. The above mentioned equation yields the value of −4.9 J/gat K

2 optional reactions can lead to the formation of CaMgSn:

1. $Ca_{0.5}Sn_{0.5} + Mg_{0.5} \rightarrow 3/2\ Ca_{0.333}Mg_{0.333}Sn_{0.334}$ with Gibbs free energy of formation of –53500 + 18.34 T J/g at
2. $Mg_{0.667}Sn_{0.333} + Ca_{0.667}Sn_{0.333} \rightarrow 2\,Mg_{0.333}Ca_{0.333}Sn_{0.334}$ with Gibbs free energy of formation of −43100 + 9.45 T J/g at

The reaction $Mg_{0.667}Sn_{0.333} + Mg_{0.667}Ca_{0.333} \rightarrow 2\ Ca_{0.167}Mg_{0.667}Sn_{0.166}$ with Gibbs energy of formation of –18400 + 2.45 T J/g at results in a potential phase $Ca_{0.167}Mg_{0.667}Sn_{0.166}$ (or $0.167CaMg_4Sn$), which is located on the tie line between pure Mg and CaMgSn. In order to permit stable Mg-CaMgSn equilibrium, the Gibbs free energy of formation of Mg + CaMgSn must be more negative than −18400 +2.45∗T J/g at, thus the first option was selected as the initial approximation.

This data was used to simulate the phases present in a Mg-Al-Ca-Sn alloy. It was calculated that the microstructure is composed of α(hcp)Mg and Mg_2Sn. However, αMg and CaMgSn were found experimentally. In order to stabilize the CaMgSn over Mg_2Sn, its Gibbs free energy of formation must be more negative, but this resulted in an unreasonable high melting point for CaMgSn. Thus the gibbs energy must increase more rapidly with temperature. Finally, −75000 + 38 T J/g at was adopted for the

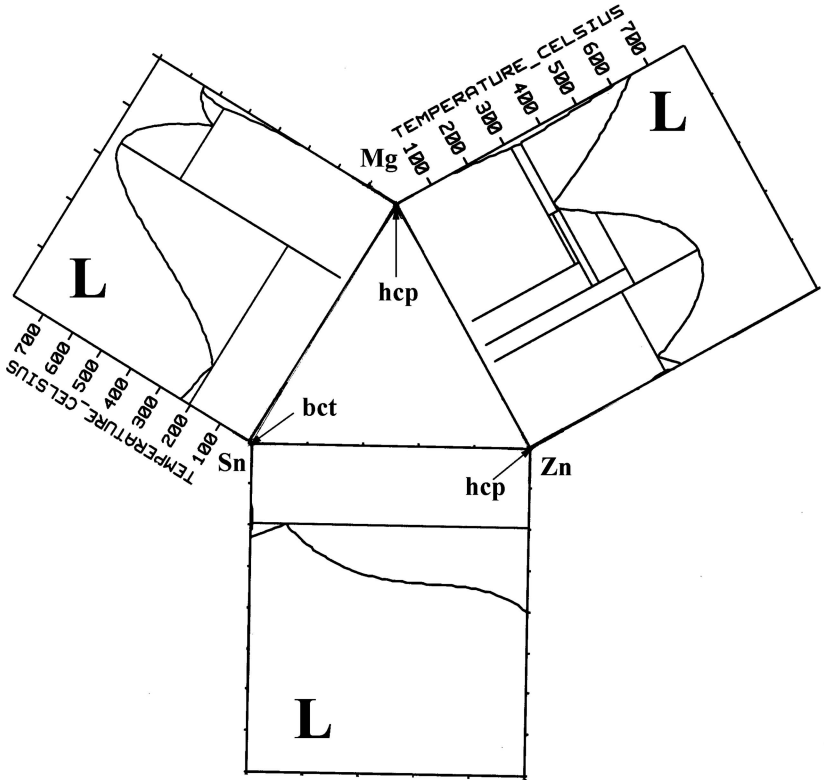

Figure 1 Calculated edge binary diagram of the Mg-Zn-Sn system.

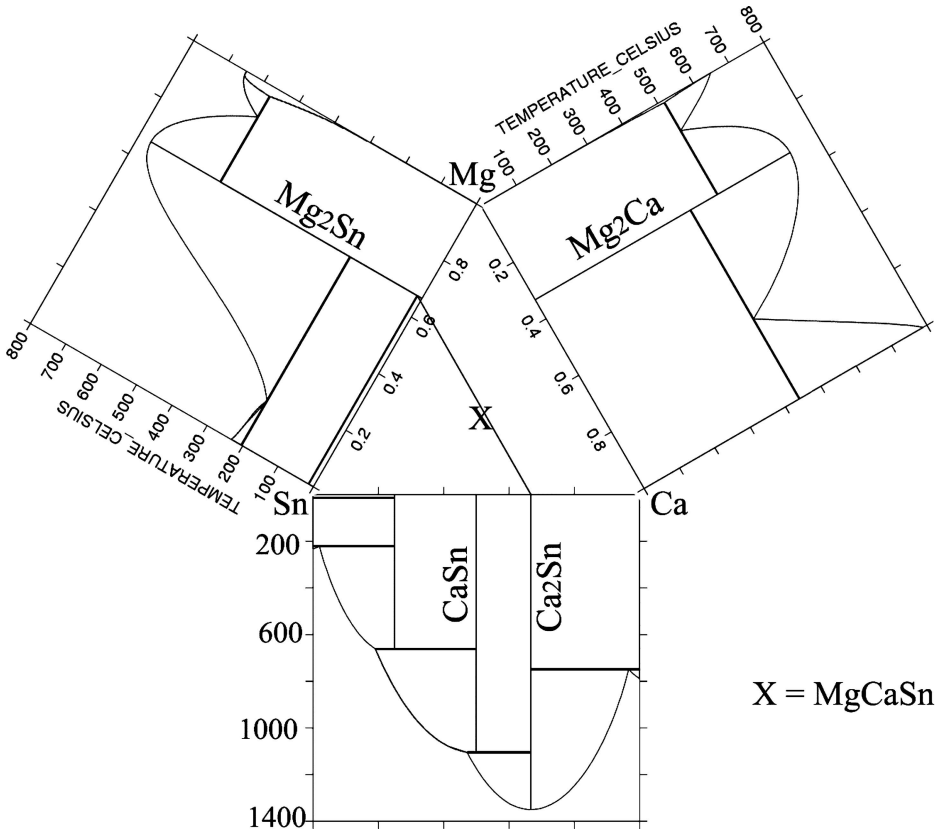

Figure 2 Isothermal cross-section at room temperature in the Mg-Ca-Sn system with the three edge binary diagrams.

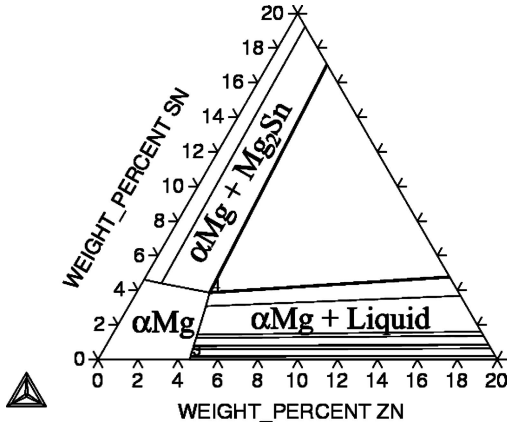

Figure 3 Isothermal section at 450°C in the Mg-Sn-Zn system.

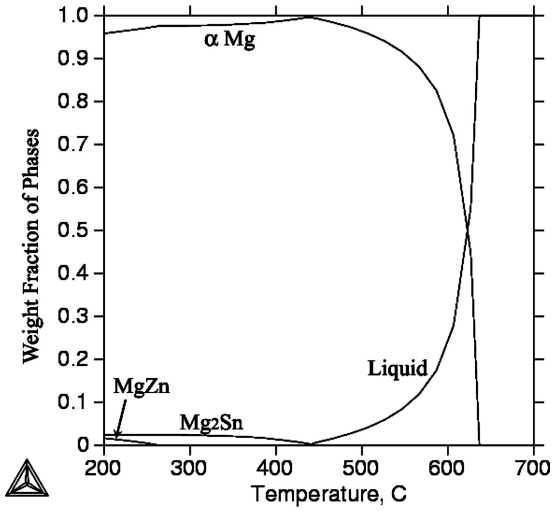

Figure 4 Weight fraction of phases in equilibrium as a function of the temperature in a Mg-3.75%Sn-4%Zn alloy.

compound phase parameter of CaMgSn.Thus the gibbs energy of this phase is thus given by Equation 5 as:

$$\begin{aligned} Ca_{0.333}Mg_{0.333}Sn_{0.334} = &-75000 + 38 * T \\ &+ 0.333 * GHSERCA \\ &+ 0.333 * GHSERMG \\ &+ 0.334 * GHSERSN \text{ J/g at} \end{aligned} \quad (5)$$

The ThermoCalc software package was used with the Mg17.R15.TDB database to calculate the equilibrium phase relations. This method was also used to calculate the phases formed during solidification and their composition based on the ThermoCalc Scheil Module.

Based on this simulation, the coexisting phases in cast alloys of the the Mg-Sn-Zn and Mg-Sn-Zn-Ca systems and their composition, as well as the solution treatment procedure, were calculated. The precipitation of minor phases in solutionized and aged samples and during the exposure to elevated temperatures of samples in the as-cast state was predicted.

3. Results

An iso-thermal section at 450°C in the Mg-Sn-Zn system was calculated, and the Mg-rich corner is presented in Fig. 3. The alloy Mg-3.75%Sn-4%Zn was selected as a heat-treatable alloy because it is located within the αMg single-phase region seen in Fig. 3.

The phases at equilibrium in this alloy as a function of the temperature are shown in Fig. 4. It can be seen that the liquidus temperature is 635°C and the solidus is about 460°C (where the weight fraction of the liquid is less than 1%), thus the mushy zone width corresponds well with values typical of commercial alloys—castability comparable to that of alloys of the AZ and AM series can be expected.

From Fig. 4 it can also be seen that Mg_2Sn precipitates slightly below 440°C and MgZn is formed at 250°C. Therefore, in the temperature range of 440–460°C only HCP αMg exists (the total weight fraction of all other phases is below 1%). Therefore, the two requirements for an heat-treatable alloy, i.e., the existence of a single phase region and the precipitation of inter-metallic compounds, are met by the selected alloy.

Based on the Scheil model for solidification, the weight fraction of the solid as a function of the temperature was calculated (see Fig. 5). It can be seen that the solidification terminates at 330°C with a eutectic reaction, which occupies about 8% of the volume.

The minor solid phases, besides HCP αMg, which are formed during the solidification and presented in Fig. 6, were calculated with the aid of the ThermoCalc software by using Scheil model for solidification. Mg_2Sn solidifies together with α(hcp)Mg, where as the grain boundary eutectic is expected to be composed of Mg and MgZn. The

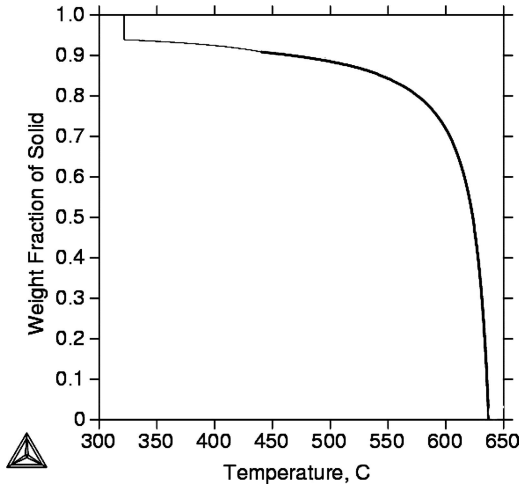

Figure 5 Weight fraction of the solid during solidification of a Mg-3.75%Sn-4%Zn alloy. The calculation is based on Scheil's model for solidification.

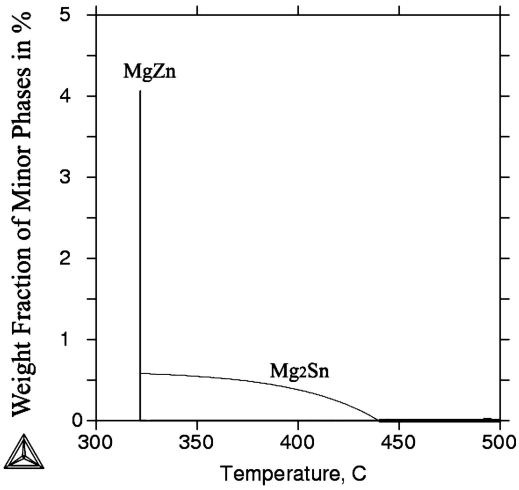

Figure 6 Calculated minor phases, besides the HCP αMg, formed during the solidification of Mg-3.75%Sn-4%Zn alloy.

as-cast microstructure seen in Fig. 7 reveals the existence of Mg_2Sn and an Mg-MgZn eutectic in the grain boundaries. Basically, the solution treatment should be carried out at a temperature range in which only one phase exists (i.e. in a single phase region). From Fig. 4 it can be concluded that an appropriate range is 440–460°C, where as Figs 5 and 6 show that the solidification terminates in a grain boundary eutectic reaction at 330°C. Namely the solution temperature is much higher than the melting temperature of the grain boundaries eutectic. Therefore, during rapid heating to the solution temperature, the low-melting eutectic on the grain boundaries will melt. In order to prevent grain-boundary melting, the samples were heated from the eutectic temperature (330°C) to the solution temperature (~ 450°C) under quasi-static conditions. This can be guaranteed by applying a very slow heating rate (i.e. 1°C/Hr) in a way that the grain boundary melting could be eliminated. After 96 h at the solution treatment temperature, water quenching provides the rapid cooling required for preserving the alloying elements in αMg solid-solution at room temperature. The XRD pattern given in Fig. 8 reveals only the existence of αMg after the solution treatment.

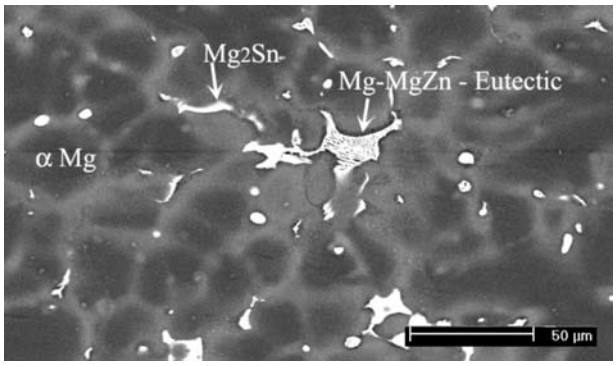

Figure 7 Microstructure in the as-cast state.

Fig. 4 shows that at 175°C, Mg_2Sn and MgZn are at equilibrium with αMg. These phases were found after aging for 96 h at 175°C (Fig. 9).

The coring effect taking place during solidification is reflected in the variation in the composition of αMg with temperature, as presented in Fig. 10. The Zn and Sn content in αMg towards the end of solidification, namely in the region close to the grain boundaries, are 6.9% and 0.3% respectively, as against 4%Zn and 3.75%Sn average content in the alloy. The coring effect is evident as bright regions seen in Fig. 7 close to the grain boundaries. The local composition mentioned above was used to calculate the weight fraction of the coexisting phases in this region as a function of temperature, as shown in Fig. 11. Only the two phases mentioned above precipitate from the αMg matrix, and it can be expected that most of the precipitation during exposure of the as-cast structure to 175°C will take place in the vicinity of the grain boundaries of the αMg matrix. Fine precipitation, mainly in the vicinity

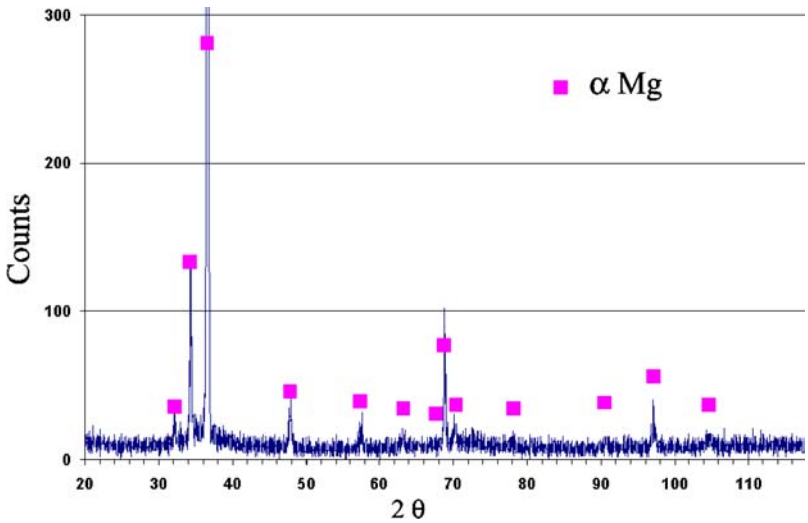

Figure 8 XRD pattern of solution treated Mg-Sn-Zn alloy.

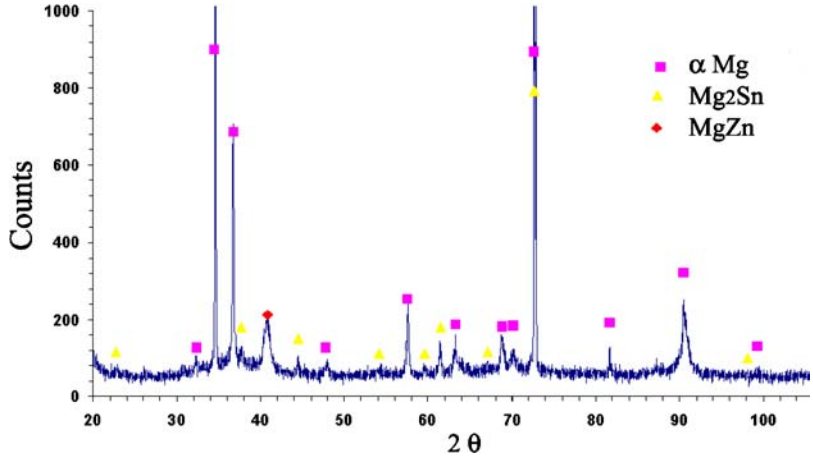

Figure 9 XRD pattern of solution treated and aged Mg-Sn-Zn alloy.

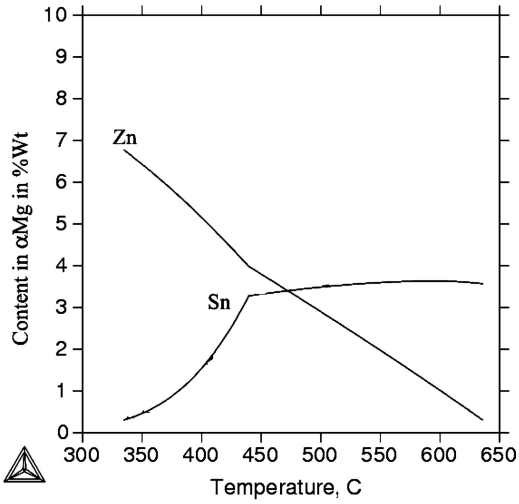

Figure 10 Calculated variation of the solidified αMg composition with temperature in a Mg-3.75%Sn-4%Zn alloy.

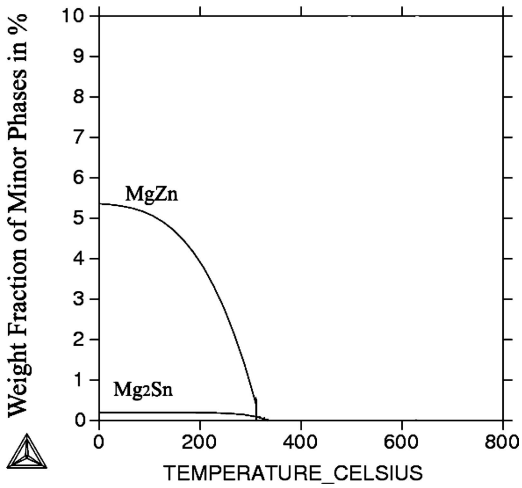

Figure 11 Weight fraction of the coexisting phases in the vicinity of the grain boundaries in a Mg-3.75%Sn-4%Zn alloy as a function of temperature.

of the grain boundaries, was indeed found experimentally (Fig. 12).

The Mg_2Ca is the only intermetallic compound in the Mg-Ca binary system, similar to the Mg_2Sn in the Mg-Sn system. Therefore, it was expected that the addition of Ca would result in additional precipitation and hence would be beneficial to improve the properties. Simulating the phases at equilibrium in an alloy modified by 1%Ca (Fig. 13) shows that at 560°C, above the solidus temperature, MgCaSn solidifies whereas Mg_2Ca does not exist at all. The two minor phases found in the base alloy discussed earlier are also presented in the modified alloy. XRD pattern of as-cast Mg-3.75%Sn-4%Zn-1%Ca (Fig. 14) reveals these findings.

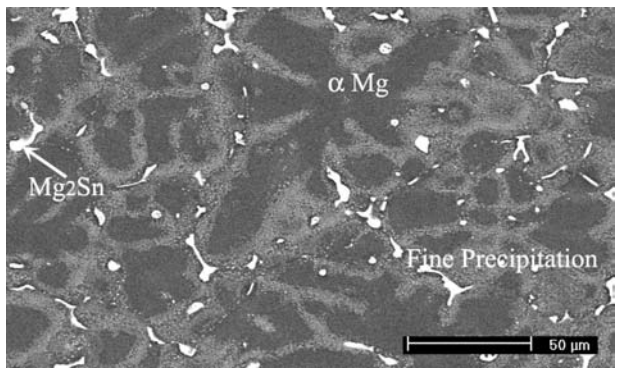

Figure 12 Microstructure of cast Mg-Sn-Zn exposed to 225 °C for 32 days.

4. Discussion

Thermodynamic calculations were used for two purposes:

1. Deepen the understanding of the phase formation and solute distribution during solidification.

2. Determine the Heat-Treatment-Window for solution treatment and aging.

These purposes are discussed in detail below.

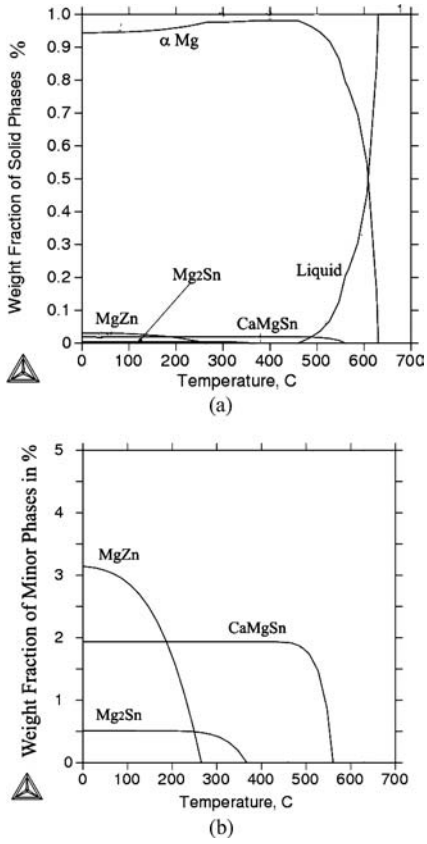

Figure 13 Weight fraction of phases in equilibrium as a function of the temperature in a Mg-3.75%Sn-4%Zn-1%Ca alloy.

4.1. Solidification

Although the liquidus and solidus temperatures of a Mg-3.75%Sn-4%Zn are 635 and 460°C respectively, the solidification, being a non-equilibrium process, terminates with an eutectic reaction Liquid → αMg + MgZn in the grain boundaries at 330°C (Figs. 4 & 5), which was verified experimentally (Fig. 7). The eutectic reaction resulted from the enrichment of the inter-dendritic residual melt by Sn and Zn, due to the segregation of the alloying elements (especially Zn) to the residual melt.

The solidification of the investigated alloy starts with the formation of αMg, followed by the solidification of Mg_2Sn from the Sn & Zn enriched liquid at 440°C (Fig. 6). This is in contrast to the solid-state precipitation of Mg_2Sn from a super-saturated αMg at equilibrium shown in Fig. 4. The formation of this phase before the solidifaction is completed will result in its presence as coarse particles on the grain boundaries, as evident in Fig. 7. In addition, this results in dilution of the melt with Sn, and accordingly the αMg regions, which solidified at temperatures below the one of Mg_2Sn formation (440°C), are Sn depleted. This is reflected in the variation in the calculated local content of Sn and Zn in αMg, as shown in Fig. 10. The regions in the vicinity of the αMg grain boundaries, which are the last to solidify, are therefore highly enriched with Zn but low on Sn. This local enrichment is manifested in the bright straps close to the grain boundaries (Fig. 7)

Based on the simulation results—eutectic temperature of 330°C and the existence of an αMg single-phase region at 440–460°C —the solution treatment procedure was established. In order to prevent grain boundary melting, the specimen were kept slightly below 330°C for 96 h, followed by quasi-stationary heating to the solution temperature of 460°C, kept at this temperature for additional 96 h followed by water quenching.

4.2. Solution treatment & aging

The foreseen αMg single-phase region, where the solution treatment was carried out, resulted in complete dissolution of the alloying elements in the αMg matrix during solution treatment and in the formation of a homogeneous structure where Zn and Sn are uniformly distributed. This was proven experimentally by the XRD pattern given in Fig. 8, which reveals the existence of αMg only.

At 440°C, Mg_2Sn starts to precipitate from the super saturated matrix, and at a lower temperature, MgZn

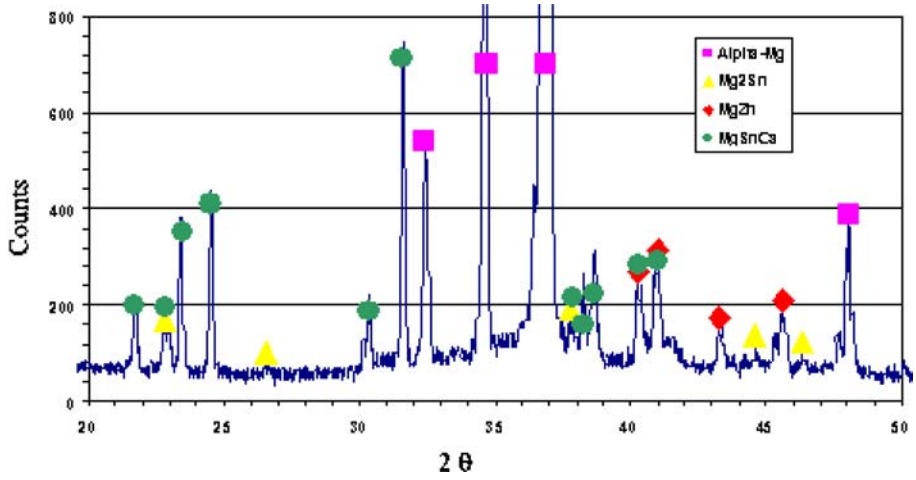

Figure 14 XRD pattern of solution treated and ages Mg-Sn-Zn-Ca alloy.

precipitates. It can be expected that below 200°C, the aging of super saturated matrix will result in double aging, as was confirmed by the XRD pattern shown in Fig. 9. Although the precipitation temperature of Mg_2Sn is higher than the one of MgZn, and hence the driving force for precipitation can be expected to be higher, the precipitation sequence during aging cannot be foreseen, since it depends mainly on kinetic factors, e.g. the availability of nucleation sites and diffusion, which are not considered by the ThermoCalc, being a thermodynamic software package.

As discussed earlier, the regions in the vicinity of the αMg grain boundaries (Fig. 10), which are the last to solidify, are therefore highly enriched with Zn but low on Sn. This, in turn, resulted mainly in the precipitation of MgZn (the expected amount of Mg_2Sn is negligible $<0.2\%$, see Fig. 11) in these regions during the exposure of the alloy to elevated temperature, discernible in Fig. 12, as fine precipitations in the vicinity of the grain boundaries. Since Mg_2Sn and MgZn are formed during solidification, the solid-state precipitation of MgZn cannot be resolved using XRD analysis.

According to the simulation, the addition of 1%Ca to the base alloy will result in the formation of the high-melting point MgCaSn compound (Fig. 13) rather than the binary Mg_2Ca. Due to its formation in an early stage of the solidification, it will be presented as relatively coarse grain-boundary phase. Therefore, this phase is not expected to contribute to the precipitation hardening. Moreover, the Sn consumed by this phase will not be dissolved in the αMg during solution treatment at a temperature below the decomposition temperature of MgCaSn (560°C). Therefore, the amount of Mg_2Sn, which can precipitate during the aging of Mg-3.75%Sn-4%Zn-1%Ca, is about 0.5% as against the expected 2.5% in the base alloy (compare Figs. 4 & 13). In conclusion, the addition of Ca will adversely affect the precipitation hardening.

The reported study demonstrates the application of the thermodynamics calculation in a more efficient design of alloys and their heat-treatment. The alloy selection and the solution treatment procedure were determined exclusively by simulation and verified experimentally. Furthermore, the simulation allows the assessment of the grain boundary phases in the as-cast structure. In this context the simulation of Mg-3.75%Sn-4%Zn-1%Ca demonstrates that the addition of Ca will NOT bring about any improvement in the precipitation hardening, due to partial consumption of Sn by MgCaSn, thereby resulting in lower hardening by Mg_2Sn precipitation. The thermodynamic calculation permits the estimation of the weight (or molar) fraction of each phase to precipitate, however kinetic aspects, like the precipitation sequence and precipitation rates, cannot, naturally, be foreseen by thermodynamic simulation. Therefore, in case of double precipitation, Thermo-Calc simulation cannot foresee which phase will be the first to form.

5. Summary

The thermoCalc software package, in conjunction with an appropriate database, was used to design heat-treatable Mg based alloys. The selection of alloy was based on the existence of an αMg single-phase region. The solution treatment procedure was determined so as to prevent grain-boundary melting due to the existence of eutectic reaction at low temperature. In addition, the simulation allows foreseeing the phases that precipitate during exposure to elevated temperature of either solution treated samples, or in the as-cast state without solution treatment. This precipitation affects, in turn, the alloy properties during service at elevated temperatures.

Acknowledgement

Dr. Larry Kaufman, Brookline, MA, USA is acknowledged for his support and fruitful discussions. This study was supported by a Grant from the GIF, the German-Israeli-Foundation for Scientific Research and Development under contract I-704-43.10/2001 and partially by the fund for the promotion of research at the Technion

References

1. Z. ZHANG, A. COUTURE and A. LUO, *Scripta Materialia* **39** (1998) 45.
2. M. P. LIU, Q. D WANG, X. Q. ZENG, Y. H. WEI, Y. P. ZHU and C. LU, *Z. Metallkunde*. **94** (2003) 886.
3. M. PEKGULERYUZ, P. LABELLE, D. ARGO and E. BARIL, "Mg Technology 2003," edited by H. I. Kaplan TMS 2003 Annual Meeting, (San Diego, USA, 2003), p. 201,
4. J. B. OK, I. J. KIM, S. YI, W. T. KIM and D. H. KIM, *Philosoph. Mag.* **83** (2003) 2359.
5. Y. GUANGYIN, L. MANPING, D. WENJIANG and A. INOUE, *Mater. Sci. Engng.* **A357** (2003) 314.
6. P. LIANG, H-L SU, P. DONNADIEU, M. G. HARMERLIN, A. QUIVY, P. OCHIN, G. EFFENBERG, H. J. SEIFERT, H. L. LUKAS and F. ALDINGER, *Z. Metallkunde*. **89** (1998) 536.
7. R. SCHMIDT-FETZER and J. GRÖBNER, in Proceedings of the 6th Int. Conference "Magnesium Alloys and their Applications 2003," edited by K. U. Kainer (DGM, Wiley-VCH, Weinheim, 2003) p. 12.
8. K. OZTURK, Y. ZHONG, Z-K LIU and A. LUO, Mg Technology 2001, edited by J. Hryn (TMS, New Orleans, USA, 2001), P. 113.
9. Y. ZHONG, K. OZTURK, Z-K LIU and A. LUO, "Mg Technology 2002," edited by H.I. Kaplan (TMS, Seattle, USA, 2002) p. 69.
10. F. VON BUCH, J. LIETZAU, B. L. MORDIKE, A. PISCH and R. SCHMID-FETZER, *Mater. Sci. Engng.* **263** (1999) 1.
11. J. GRÖBNER, D. KEVORKOV and R. SCHMID-FETZER, *Intermetallics* **10** (2002) 415.
12. C. O. BRUBAKER and Z-K. LIU, *J. Alloys Comp.* **370** (2004) 114.
13. J. GRÖBNER, I. CHUMAK and R. SCHMID-FETZER, *Intermetallics* **11** (2003) 1065.
14. K. OZTURK, Z-K. LIU and A. LUO, "Mg Technology 2003," edited by H. I. Kaplan TMS 2003 Annual Meeting, (San Diego, USA, 2003) p.195.
15. H. LIANG, S. L. CHEN and Y. A. CHANG, *Metallurg. Trans.* **28A** (1997) 1725.
16. J. GRÖBNER, D. KEVORKOV, I. CHUMAK and R. SCHMID-FETZER, *Z. Metallkunde* **94** (2003) 976.

17. "Magnesium Taschenbuch," edited by C. Kammer (Aluminium-Verlag GmbH Düsseldorf, 2000) p. 171.
18. P. R. Beeley, Foundry Technology, Butterworths, London 1972.
19. Dead Sea Magnesium — Patent Pending, Private Communication.
20. T. DINSDALE, *CALPHAD* **15** (1991), 317.
21. R. HULTGREN, P. D. DESAI, D. T. HAWKINS, M. GLEISER and K. K. KELLEY ASM, Cleveland, Metals Park Ohio (1973).
22. T. B. MASSALSKI, J. L. MURRAY, L. H. BENNETT and H. BAKER ASM, Cleveland, Metals Park Ohio (1996).
23. A. A. NAYEB-HASHEMI and J. B. CLARK, *Results*: *Bulletin of Alloy Phase Diagrams* **5** (1984) 456.
24. A. A. NAYEB-HASHEMI and J. B. CLARK, *ibid* **8** (1987) 58.
25. M. MORISHITA and K. KOYAMA *J. Alloys Comp.* **398** (2005) 12.

Received 27 February
and accepted 19 August 2005